

Computing Periodic Orbits of Nondifferentiable/Discontinuous Mappings Through Particle Swarm Optimization

K.E. Parsopoulos and M.N. Vrahatis

Department of Mathematics

University of Patras Artificial Intelligence Research Center (UPAIRC)

GR-26110 Patras, Greece

Email: {kostasp, vrahatis}@math.upatras.gr

Abstract—Periodic orbits of nonlinear mappings play a central role in the study of dynamical systems. Traditional root finding algorithms, such as the Newton–family algorithms, have been widely applied for the detection of periodic orbits. However, in the case of discontinuous/nondifferentiable mappings and mappings with poorly behaved partial derivatives, this approach is not valid. In such cases, stochastic optimization algorithms have proved to be a valuable tool. In this paper, a new approach for computing periodic orbits through Particle Swarm Optimization, is introduced. The results indicate that the algorithm is robust and efficient. Moreover, the method can be combined with established techniques, such as Deflection, to detect several periodic orbits of a mapping. Finally, the minor effort which is required to implement the proposed approach, renders it an efficient alternative for computing periodic orbits of nonlinear mappings.

I. INTRODUCTION

Nonlinear mappings can be used to model conservative or dissipative dynamical systems [1]–[13]. Central role in the analysis of such mappings is played by points, which are invariant under the mapping, called *fixed points* or *periodic orbits* [13]. A point

$$X = (x_1, \dots, x_n)^\top \in \mathbb{R}^n,$$

is called *fixed point* of a mapping

$$\Phi(X) = (\Phi_1(X), \dots, \Phi_n(X))^\top : \mathbb{R}^n \rightarrow \mathbb{R}^n,$$

if $\Phi(X) = X$, and it is called a *fixed point of order p* , or a *periodic orbit of period p* , if

$$X = \Phi^p(X) \equiv \underbrace{\Phi(\Phi(\dots(\Phi(X))\dots))}_{p \text{ times}}. \quad (1)$$

Detecting periodic orbits of nonlinear mappings is one of the most challenging problems of nonlinear science, since analytic expressions for evaluating periodic orbits can be obtained only if the mapping is a polynomial of low degree and the period is low. Traditional methods, such as the Newton–family methods and related classes of algorithms, often fail, as they are affected by the mapping evaluations assuming large values in the neighborhood of *saddle–hyperbolic* periodic orbits, which are *unstable* in the linear approximation. The failure

of these methods can also be attributed to the nonexistence of derivatives or poorly behaved partial derivatives in the neighborhood of the fixed points.

Swarm Intelligence methods are stochastic optimization, machine learning and classification systems, that model intelligent behavior. They are intimately related to the field of Evolutionary Computation, which consists of algorithms motivated from biological genetics and natural selection. A common characteristic of all these algorithms, is the exploitation of a population of search points to probe the search space simultaneously. Particle Swarm Optimization (PSO) belongs to the category of Swarm Intelligence methods. The dynamic of the population resembles the collective behavior and self–organization of socially intelligent organisms [14]. The individuals of the population exchange information and benefit from their discoveries as well as the discoveries of other companions, while exploring promising areas of the search space. In the minimization context, such areas possess low function values.

In this paper, a new efficient numerical method for computing periodic orbits of nonlinear mappings is introduced. This method is based on the minimization of a nonnegative objective function through PSO. The objective function is constructed so that its global minimizers constitute the periodic orbits of a specific period p , of the original mapping. Thus, detecting the global minimizers of the objective function is equivalent to computing the periodic orbits of period p . To detect several periodic orbits of the desired period, the Deflection technique is applied.

The rest of the paper is organized as follows: the PSO algorithm is briefly described in Section II. In Sections III and IV, the Deflection technique, for detecting several minimizers of a function, as well as the proposed approach for the detection of periodic orbits, are described, respectively. The experimental results are reported in Section V, and conclusions are derived in Section VI.

II. THE PARTICLE SWARM OPTIMIZATION ALGORITHM

PSO is a stochastic machine learning, optimization algorithm [14]–[17]. The ideas that underlie PSO are inspired not

by the evolutionary mechanisms encountered in natural selection, but rather by the social dynamics of flocking organisms, such as swarms, which are governed by fundamental rules like nearest-neighbor velocity matching and acceleration by distance [15], [17].

PSO is a population based algorithm, i.e., it exploits a population of individuals to probe promising regions of the search space simultaneously. In this context, the population is called *swarm* and the individuals (i.e., the search points) are called *particles*. Each particle moves with an adaptable velocity within the search space, and retains a memory of the best position it ever encountered, i.e., the position of the search space that possesses the lowest function value so far. In the *global* variant of PSO, the best position ever attained by all individuals of the swarm is communicated to all the particles. In the *local* variant, each particle is assigned to a neighborhood consisting of a prespecified number of particles. In this case, the best position ever attained by the particles that comprise the neighborhood is communicated among them [17]. The present paper, considers the global variant of PSO only.

Assume a n -dimensional search space, $S \subset \mathbb{R}^n$, and a swarm consisting of N particles. Each particle is in effect a n -dimensional vector,

$$X_i = (x_{i1}, x_{i2}, \dots, x_{in})^\top \in S, \quad i = 1, \dots, N.$$

The velocities of the particles are also n -dimensional vectors,

$$V_i = (v_{i1}, v_{i2}, \dots, v_{in})^\top, \quad i = 1, \dots, N.$$

The best previous position encountered by the i -th particle is a point in S , denoted by

$$P_i = (p_{i1}, p_{i2}, \dots, p_{in})^\top \in S.$$

Let g be the index of the particle that attained the best previous position among all the individuals of the swarm, i.e.

$$f(P_g) \leq f(P_i), \quad i = 1, \dots, N,$$

where f is the objective function under consideration. Then, the swarm is manipulated according to the equations [18]:

$$V_i^{(t+1)} = \chi \left(V_i^{(t)} + c_1 r_1 (P_i^{(t)} - X_i^{(t)}) + c_2 r_2 (P_g^{(t)} - X_i^{(t)}) \right), \quad (2)$$

$$X_i^{(t+1)} = X_i^{(t)} + V_i^{(t+1)}, \quad (3)$$

where $i = 1, 2, \dots, N$; χ is a parameter called *constriction factor*; c_1 and c_2 are two fixed, positive parameters called *cognitive* and *social* parameter respectively; r_1, r_2 , are random numbers uniformly distributed in the interval $[0, 1]$; and t , stands for the counter of iterations. Alternatively, the following relation can be used for the update of velocities, instead of Eq. (2) [19]–[21]:

$$V_i^{(t+1)} = w V_i^{(t)} + c_1 r_1 (P_i^{(t)} - X_i^{(t)}) + c_2 r_2 (P_g^{(t)} - X_i^{(t)}), \quad (4)$$

where w is a parameter called *inertia weight*. Both the constriction factor and the inertia weight are used as mechanisms to control and adjust the magnitude of the velocities, to alleviate the problem of swarm explosion and divergence [22]. Often, a threshold V_{max} on the absolute value of the velocity, is incorporated, in addition to the aforementioned parameters.

The inertia weight, w , in Eq. (4), is employed to manipulate the impact of the previous history of velocities on the current velocity. Therefore, w resolves the trade-off between the global (wide-ranging) and local (nearby) exploration ability of the swarm. A large inertia weight encourages global exploration (moving to previously not encountered areas of the search space), while a small one promotes local exploration, i.e., fine-tuning the current search area. A suitable value for w provides the desired balance between the global and local exploration ability of the swarm, and consequently improves the effectiveness of the algorithm. Experimental results suggest that it is preferable to initialize the inertia weight to a large value, giving priority to global exploration of the search space, and gradually decrease it, so as to obtain refined solutions [20], [21]. This finding is intuitively appealing. In conclusion, an initial value of w around 1 and a gradual decline towards 0 is considered a proper choice for w . On the other hand, the value of the constriction factor is typically obtained through the formula [18]:

$$\chi = \frac{2\kappa}{|2 - \phi - \sqrt{\phi^2 - 4\phi}|}, \quad (5)$$

for $\phi > 4$, where $\phi = c_1 + c_2$, and $\kappa = 1$. Different configurations of χ , as well as a theoretical analysis of the derivation of Eq. (5), can be found in [18], [23]. The constriction factor version of PSO has proved to be considerably faster than the inertia weight one.

Proper fine-tuning of the parameters c_1 and c_2 , results in faster convergence and alleviation of local minima. An extended study of the acceleration parameter c , in the primary version of PSO, is provided in [24]. As default values, $c_1 = c_2 = 2$ have been proposed, but experimental results indicate that alternative configurations, depending on the problem at hand, can produce superior performance [16], [18], [23], [25].

The swarm and the velocities are randomly initialized, following a uniform distribution, within the search space. However, more sophisticated initialization techniques can enhance the overall performance of the algorithm [16], [26]. For uniform random initialization in a multidimensional search space, a Sobol Sequence Generator can be used [27].

III. DETECTING FURTHER MINIMIZERS THROUGH DEFLECTION

PSO is able to detect one, in general arbitrary, minimizer of the objective function, per run. However, in some applications, several minimizers of the objective function are required. Restarting the algorithm does not guarantee the detection of a different minimizer. In such cases, the *Deflection* technique can be used. This technique imposes a transformation of the

objective function f , once a minimizer X_i^* , $i = 1, \dots, n_{min}$, has been detected [28]:

$$F(X) = T_i(X; X_i^*, \lambda_i)^{-1} f(X), \quad (6)$$

with

$$T_i(X; X_i^*, \lambda_i) = \tanh(\lambda_i \|X - X_i^*\|), \quad (7)$$

where λ_i , $i = 1, \dots, n_{min}$, are nonnegative relaxation parameters, and n_{min} is the number of the detected minimizers. The transformed function has exactly the same minimizers with the original f , with the exception of X_i^* . Alternative configurations of the parameter λ result in different shapes of the transformed function. For larger values of λ the impact of the Deflection technique on the objective function is relatively mild. On the other hand, using $0 < \lambda < 1$ results in a function F with considerably larger function values in the neighborhood of the deflected minimizer. The effect of the Deflection procedure on the function $f(x) = \cos^2(x) + 0.1$, at the point $x^* = \frac{\pi}{2}$, is illustrated in Fig. 1

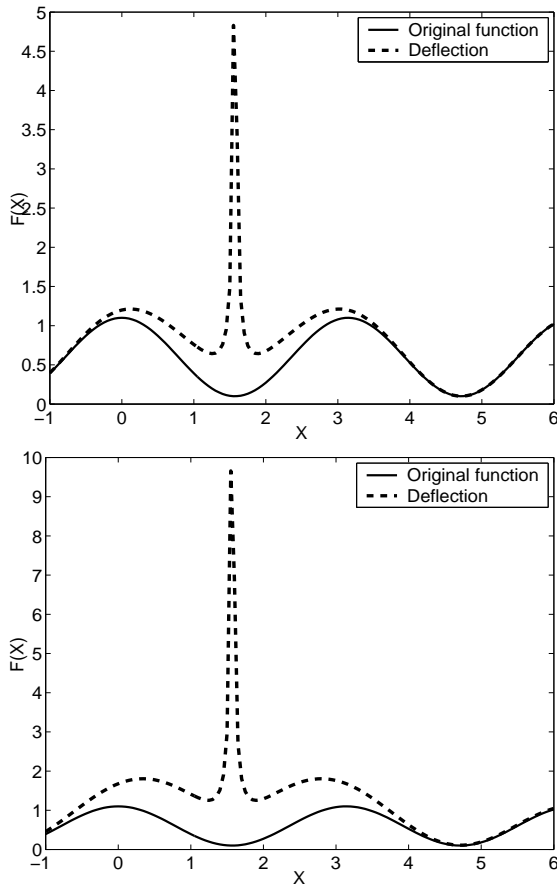


Fig. 1. The effect of the Deflection procedure on the function $f(x) = \cos^2(x) + 0.1$, at the point $x^* = \frac{\pi}{2}$, for $\lambda = 1$ (up), and $\lambda = 0.5$ (down). Note the change in the scaling of the two figures.

A point to notice is that the Deflection technique should not be used on its own on a function f , whose global minimum is zero. The reason is that the transformed function, F , of Eq. (6), will also have zero value at the deflected global minimizer,

since f will be equal to zero at such points. This problem can be easily alleviated by taking $\hat{f} = f + c$, where $c > 0$ is a constant, instead of f . The function \hat{f} possesses all the information regarding the minimizers of f , but the global minimum is increased from zero to c . The value of c does not affect the performance of the algorithm and, thus, if no information regarding the global minimum of f is available, it can be selected to be arbitrarily large.

IV. THE PROPOSED APPROACH

Let

$$\Phi(X) = (\Phi_1(X), \dots, \Phi_n(X))^T : \mathbb{R}^n \rightarrow \mathbb{R}^n,$$

be a nonlinear mapping,

$$X = (x_1, \dots, x_n)^T \in \mathbb{R}^n,$$

be a periodic orbit of period p of Φ , and $\Theta_n = (0, \dots, 0)^T$ be the origin of \mathbb{R}^n . Then, by definition, the following relation holds:

$$\begin{aligned} \Phi^p(X) = X &\Rightarrow \Phi^p(X) - X = \Theta_n \Rightarrow \\ \begin{pmatrix} \Phi_1^p(X) \\ \vdots \\ \Phi_n^p(X) \end{pmatrix} - \begin{pmatrix} x_1 \\ \vdots \\ x_n \end{pmatrix} &= \begin{pmatrix} 0 \\ \vdots \\ 0 \end{pmatrix} \Rightarrow \\ \begin{cases} \Phi_1^p(X) - x_1 = 0, \\ \vdots \\ \Phi_n^p(X) - x_n = 0. \end{cases} & \end{aligned} \quad (8)$$

We can define, now, an objective function f ,

$$f(X) = \sum_{i=1}^n (\Phi_i^p(X) - x_i)^2, \quad (9)$$

which is nonnegative, and its global minimizers, for which $f(X) = 0$, are periodic orbits of period p of the mapping Φ . Thus, globally minimizing f is equivalent to computing the periodic orbits of period p of Φ .

The shape of the objective function f heavily depends on the mapping Φ . If Φ is continuous and differentiable, then the minimization can be effectively performed through gradient-based techniques. Many applications, however, involve discontinuous/nondifferentiable mappings. In such cases, stochastic optimization algorithms, that require function values solely, can be applied.

The proposed approach involves the minimization of the objective function f , through the PSO algorithm. Possible discontinuities of f do not affect its convergence. In Figs. 2 and 3 the phase plot as well as the contour plot of the obtained function f for the 2-dimensional Hénon map, are exhibited, for $\cos \alpha = 0.24$ and $\cos \alpha = 0.8$ respectively, while the 3-dimensional plot of the obtained f for the Standard Map, as well as, its contour plot are displayed in Fig. 4 (the definitions of the aforementioned mappings are given in Section V). In the latter case, the multitude of discontinuities, precludes the use of a deterministic optimization algorithm for the minimization of f .

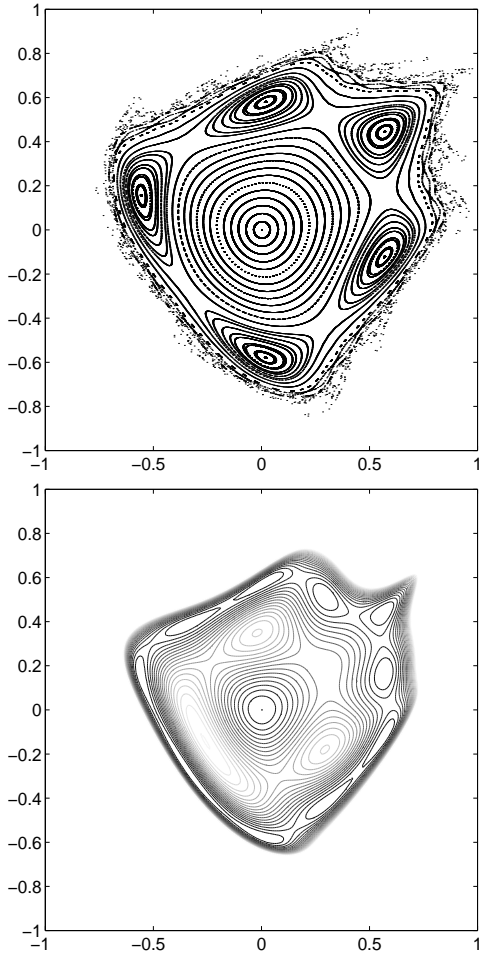


Fig. 2. Phase plot of the Hénon map for $\cos \alpha = 0.24$ (up) and the contour plot of the corresponding objective function for $p = 5$ (down). Darker lines denote lower function values.

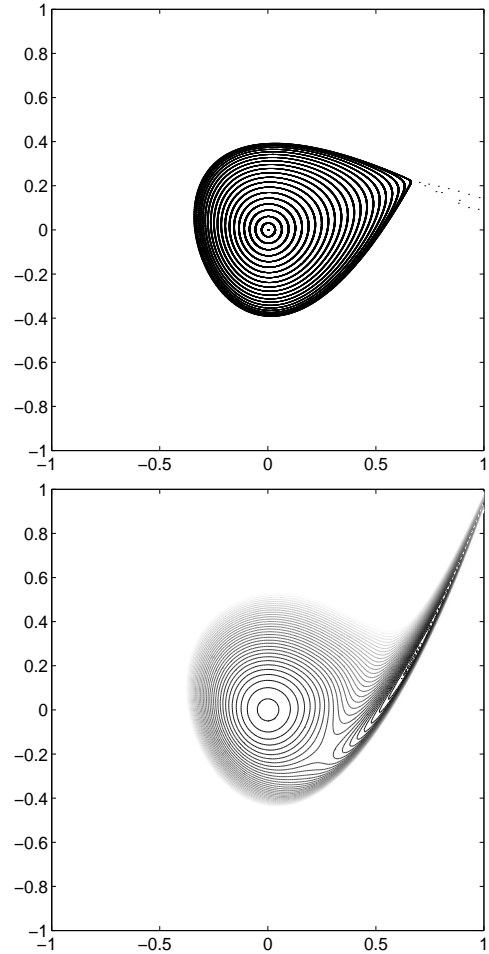


Fig. 3. Phase plot of the Hénon map for $\cos \alpha = 0.8$ (up) and the contour plot of the corresponding objective function for $p = 1$ (down). Darker lines denote lower function values.

Let X^* be a global minimizer of f and, thus, periodic orbit of period p of Φ . The stability of X^* can be determined through established techniques [29], [30]. The several types of an unstable orbit are exhibited and discussed in [30]. The rest $p - 1$ periodic orbits of the same period and type can be obtained through $p - 1$ subsequent iterations of the mapping Φ on X^* . Periodic orbits of the same period, but different stability type, can be obtained by applying the Deflection technique on the already detected periodic orbits, and then apply the PSO algorithm on the deflected function. The proposed algorithm is described in pseudocode in Table I.

A periodic orbit of period 1 is also periodic orbit of any period $p > 1$. The problem of detecting periodic orbits of period 1, instead of periodic orbits of the desired period, can also be alleviated through the application of Deflection on such a periodic orbit, as soon as it is detected.

V. EXPERIMENTAL RESULTS

In this section, the performance of PSO, is investigated on different test problems. The *constriction factor* version of PSO has been used. This choice was based solely on the faster

convergence rates that characterize it, as well as the promising results attained through it. In previous work, the *inertia weight* version was used, in some of the test problems presented here, with promising results, though the required computational time was larger [31]. Default optimal values of the PSO's parameters, which are used widely in the literature, have been used: $\chi = 0.729$, $c_1 = c_2 = 2.05$. As stopping criterion of the algorithm, the detection of the global minimum of the objective function, with an accuracy of 10^{-10} , has been used. The swarm's size is problem dependent, thus, it has been set to different values regarding the problem at hand. Moreover, whenever Deflection has been used, the objective function has been subjected to a "lift" by a parameter $c = 1$, to alleviate its disability to work properly on functions with global minimum equal to zero, as it has been described in Section III. For each test problem, periodic orbits of different periods as well as the corresponding required number of iterations are reported.

TEST PROBLEM 1. [1], [6], [7] (Hénon 2-dimensional map)

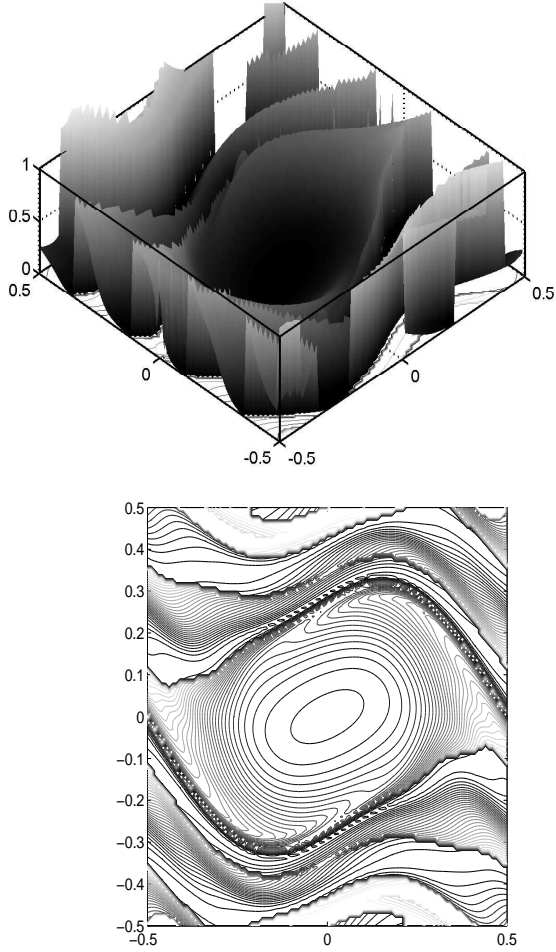


Fig. 4. 3-dimensional plot (up) and contour plot (down) of the objective function f for the Standard Map and period $p = 5$. Darker lines denote lower function values.

This mapping is defined by the following equation:

$$\Phi(X) = \begin{pmatrix} \cos \alpha & -\sin \alpha \\ \sin \alpha & \cos \alpha \end{pmatrix} \begin{pmatrix} x_1 \\ x_2 - x_1^2 \end{pmatrix} \Leftrightarrow \begin{cases} \Phi_1(X) = x_1 \cos \alpha - (x_2 - x_1^2) \sin \alpha, \\ \Phi_2(X) = x_1 \sin \alpha + (x_2 - x_1^2) \cos \alpha, \end{cases}$$

where $\alpha \in [0, \pi]$ is the rotation angle. The corresponding phase plots for $\cos \alpha = 0.24$ and $\cos \alpha = 0.8$, as well as the contour plot of the obtained objective function for $p = 5$ in the first case and for $p = 1$ in the latter case, in $[-1, 1]^2$, are displayed in Figs. 2 and 3, respectively.

The objective function for $\cos \alpha = 0.8$ and $p = 1$ has two global minimizers, one at the origin, and another in a narrow channel at the right part of the contour plot, which corresponds to a hyperbolic fixed point [1]. Due to the shape of its basin of attraction, it is difficult to detect the latter fixed point through a deterministic algorithm, unless an initial point is selected in its close vicinity. The proposed technique has been applied on this mapping for the detection of both fixed points. After the detection of the first (which can be any of the

TABLE I
THE PROPOSED ALGORITHM.

Input:	Mapping Φ , period p , desired number of deflections K .
Step 1	Set the stopping flag, $SF \leftarrow 0$, and the counter, $k \leftarrow 0$.
Step 2	While ($SF = 0$) Do Apply PSO
Step 3	If (PSO detected a solution X_1) Then Compute all points of the same type and period, X_2, \dots, X_p , by iterating the map.
Step 4	If ($k < K$) Then Apply Deflection on X_1, \dots, X_p , and set the counter $k \leftarrow k + 1$. Else Set $SF \leftarrow 1$ End If
	Else Write "No further solution was detected" Set $SF \leftarrow 1$ End If
	End While
Step 5	Report all detected solutions (if any).

TABLE II
PERIODIC ORBITS OF THE HÉNON MAP.

$\cos \alpha$	Period	Periodic Orbit	Iterations
0.8	1	(0.6666755407, 0.2222243088) ^T	56
	1	(0.0000147632, 0.0000051785) ^T	46
0.24	1	(0.0000064371, 0.0000043425) ^T	55
	5	(0.5696231776, 0.1622612843) ^T	54
	5	(0.5672255008, -0.1223401431) ^T	47
	11	(-0.4817107655, 0.6091676453) ^T	57
	43	(0.2576802556, 0.0196850254) ^T	61
	97	(0.2310634711, 0.3622185202) ^T	59
	131	(0.4173023935, 0.0842137784) ^T	58
	149	(0.2232720401, 0.2588270953) ^T	68

two fixed points), Deflection is applied and a new run starts on the deflected function. In all experiments the swarm size has been set to 150. Periodic orbits of different periods, detected through the proposed technique, as well as the corresponding required number of iterations, are reported in Table II.

TEST PROBLEM 2. [32] (Standard Map) This mapping is discontinuous and it is defined by the following equation:

$$\begin{cases} \Phi_1(X) = (x_1 + x_2 - \frac{k}{2\pi} \sin(2\pi x_1)) \bmod \frac{1}{2}, \\ \Phi_2(X) = (x_2 - \frac{k}{2\pi} \sin(2\pi x_1)) \bmod \frac{1}{2}, \end{cases}$$

where $k = 0.9$, and

$$y \bmod \frac{1}{2} = \begin{cases} (y \bmod 1) - 1, & \text{if } (y \bmod 1) > \frac{1}{2}, \\ (y \bmod 1) + 1, & \text{if } (y \bmod 1) < -\frac{1}{2}, \\ (y \bmod 1), & \text{otherwise.} \end{cases}$$

PSO has been applied on this mapping, using the same parameters as for the Hénon mapping, and results are reported in Table III.

TEST PROBLEM 3. [33] (Gingerbreadman Map) This nondifferentiable mapping is defined by the following equations:

$$\begin{cases} \Phi_1(X) = 1 - x_2 + |x_1|, \\ \Phi_2(X) = x_1, \end{cases}$$

TABLE III
PERIODIC ORBITS OF THE STANDARD MAP.

Period	Periodic Orbit	Iterations
1	(0.0000045887, 0.0000096912) ^T	23
1	(-0.5000026466, 0.0000120344) ^T	59
1	(0.4999933014, 0.0000017242) ^T	58
3	(-0.4999915291, -0.2868650976) ^T	53
3	(-0.2131328591, 0.2868633426) ^T	71
3	(-0.0000024632, -0.3684546911) ^T	116
5	(-0.2923354168, -0.2923810215) ^T	132
5	(-0.2924003042, 0.1541390546) ^T	140
5	(0.3283008215, -0.3434730122) ^T	62
5	(-0.4150743537, 0.3422455741) ^T	57

TABLE IV
PERIODIC ORBITS OF THE GINGERBREADMAN MAP.

Period	Periodic Orbit	Iterations
1	(1.0000108347, 1.0000061677) ^T	73
5	(-1.0000047942, 3.0000114057) ^T	71
5	(3.0000036048, 0.9999987183) ^T	82
6	(0.3844633827, 0.7140403542) ^T	1

and its phase plot, as well as the contour plot of the corresponding objective function, for $p = 5$, are displayed in Fig. 5.

Each point of the interior of the central hexagon, which is displayed in the phase plot of Fig. 5, is a periodic orbit of period 6. There is also a unique periodic orbit of period $p = 1$. The proposed technique has been applied in the range $[-4, 8]^2$ and results are reported in Table IV. Note that periodic orbits of period 6 have been detected in a single iteration, since the population is uniformly initialized in the range under consideration, and almost always there are points generated in the interior of the central hexagon.

TEST PROBLEM 4. [34] (Predator–Pray Map) This mapping is defined by the following equations:

$$\begin{cases} \Phi_1(X) = \alpha x_1(1 - x_1) - x_1 x_2, \\ \Phi_2(X) = \beta x_1 x_2, \end{cases}$$

where $\alpha = 3.6545$ and $\beta = 3.226$ [35]. The proposed technique has been applied in the range $[-2, 2]^2$ and results are reported in Table V.

TEST PROBLEM 5. [36] (Lorenz Map) This mapping is defined

TABLE V
PERIODIC ORBITS OF THE PREDATOR–PRAY MAP.

Period	Periodic Orbit	Iterations
1	(0.7263613548, 0.0000047179) ^T	69
1	(0.3099830255, 1.5216605764) ^T	51
1	(0.0000008620, 0.0000033184) ^T	56
2	(0.8756170073, -0.0000020728) ^T	61

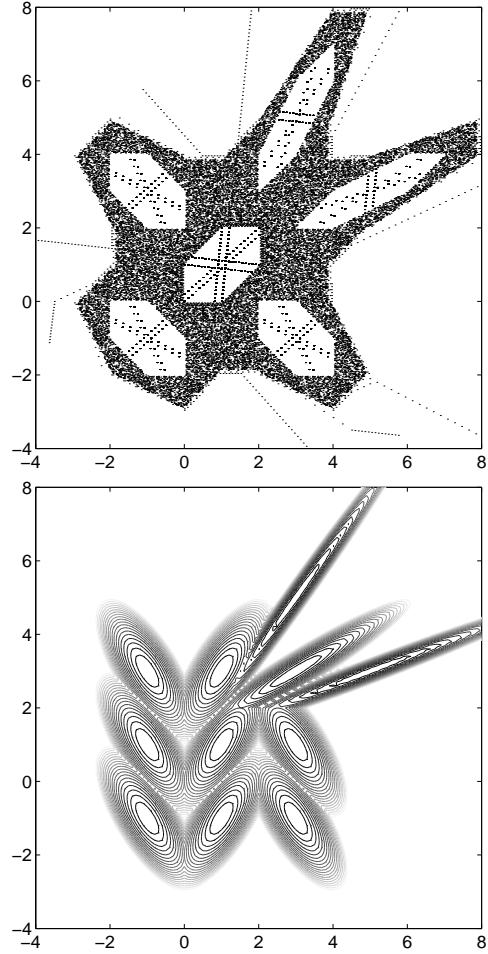


Fig. 5. Phase plot of the Gingerbreadman map (up) and the contour plot of the corresponding objective function for $p = 5$ (down). Darker lines denote lower function values.

by the following equations:

$$\begin{cases} \Phi_1(X) = \sigma(x_2 - x_1), \\ \Phi_2(X) = rx_1 - x_2 - x_1 x_3, \\ \Phi_3(X) = x_1 x_2 - bx_3, \end{cases}$$

where σ , r , and b , are the system's parameters. Lorenz took $\sigma = 10$, $b = \frac{8}{3}$. For the parameter r , the value $r = 28$ has been used [35]. There is a unique periodic orbit of period $p = 1$, in the range $[-9, 9]^3$. Applying the proposed technique, the periodic orbit

$X_1^1 = (0.0000000203, -0.0000001703, -0.0000026306)^T$, is computed after 135 iterations.

TEST PROBLEM 6. [37] (Rössler Map) This mapping is defined by the following equations:

$$\begin{cases} \Phi_1(X) = -(x_1 + x_2), \\ \Phi_2(X) = x_1 + ax_2, \\ \Phi_3(X) = b + x_3(x_1 - c), \end{cases}$$

where a , b , and c , are the system's parameters. The values $a = b = 0.2$ and $c = 5.7$ have been used [35]. Unlike the

Lorenz map, the fixed point is not at the origin, but at the point

$$X_1^1 = (-0.0132365558, -0.0165516360, 0.0297928545)^\top,$$

and it has been computed after 115 iterations.

TEST PROBLEM 7. [1], [12], [38] (Hénon 4–dimensional symplectic map) This 4–dimensional map is an extension of the Hénon 2D map to the complex case:

$$\begin{pmatrix} \Phi_1(X) \\ \Phi_2(X) \\ \Phi_3(X) \\ \Phi_4(X) \end{pmatrix} = \begin{pmatrix} R(\alpha) & \mathcal{O} \\ \mathcal{O} & R(\alpha) \end{pmatrix} \begin{pmatrix} x_1 \\ x_2 - x_1^2 + x_3^2 \\ x_3 \\ x_4 - 2x_1x_3 \end{pmatrix},$$

where α is the rotation angle, and $R(\alpha)$, \mathcal{O} , are defined as [1]:

$$R(\alpha) = \begin{pmatrix} \cos \alpha & -\sin \alpha \\ \sin \alpha & \cos \alpha \end{pmatrix}, \quad \mathcal{O} = \begin{pmatrix} 0 & 0 \\ 0 & 0 \end{pmatrix}.$$

This map can also be generalized to a symplectic map with two frequencies, α_1 and α_2 , as follows:

$$\begin{pmatrix} \Phi_1(X) \\ \Phi_2(X) \\ \Phi_3(X) \\ \Phi_4(X) \end{pmatrix} = \begin{pmatrix} R(\alpha_1) & \mathcal{O} \\ \mathcal{O} & R(\alpha_2) \end{pmatrix} \begin{pmatrix} x_1 \\ x_2 + x_1^2 - x_3^2 \\ x_3 \\ x_4 - 2x_1x_3 \end{pmatrix}.$$

The proposed technique has been applied for $\alpha = \cos^{-1}(0.24)$, with a swarm of size 400. Results are reported in Table VI.

TEST PROBLEM 8. [10], [39] This 6–dimensional map is the $n = 3$ case of the standard maps studied by Kantz and Grassberger, and it is defined by the following equations:

$$\begin{cases} x'_1 = x_1 + x'_2 \\ x'_2 = x_2 + \frac{K}{2\pi} \sin(2\pi x_1) - \frac{\beta}{2\pi} \{ \sin[2\pi(x_5 - x_1)] + \sin[2\pi(x_3 - x_1)] \} \\ x'_3 = x_3 + x'_4 \\ x'_4 = x_4 + \frac{K}{2\pi} \sin(2\pi x_3) - \frac{\beta}{2\pi} \{ \sin[2\pi(x_1 - x_3)] + \sin[2\pi(x_5 - x_3)] \} \\ x'_5 = x_5 + x'_6 \\ x'_6 = x_6 + \frac{K}{2\pi} \sin(2\pi x_5) - \frac{\beta}{2\pi} \{ \sin[2\pi(x_3 - x_5)] + \sin[2\pi(x_1 - x_5)] \} \end{cases} \pmod{1}.$$

All variables are given (mod 1), so $x_i \in [0, 1)$, for $i = 1, \dots, 6$. For $\beta = 0$, the map gives three uncoupled standard maps, while for $\beta \neq 0$ the maps are coupled and influence each other. In our experiments, $\beta = K = 1$. Results are reported in Table VII.

VI. CONCLUSIONS

The Particle Swarm Optimization method has been applied to detect periodic orbits of nonlinear mappings. The technique is based on the consideration of the problem of detecting periodic orbits, as a global minimization problem, through a proper nonnegative objective function. The global minimizers of this function coincide with the periodic orbits of a specific period. In contrast to traditional approaches, Newton–family methods, the method is capable of computing periodic orbits of nondifferentiable/discontinuous mappings.

Preliminary results on well–known and widely used nonlinear mappings indicate that PSO is efficient. Periodic orbits of different periods have been obtained rapidly. Moreover, the algorithm is easily implemented in a few lines and can be combined with the Deflection technique, to avoid the computation of already detected periodic orbits.

In the experiments reported in the previous section, the global variant of the constriction factor version of PSO has been applied. The inertia weight variant may also be successfully used, although experience indicates that for the specific task this variant exhibits worse convergence rates. The algorithm may become even faster if a particle is initialized close to an orbit. As previously mentioned, the method does not require derivatives and, thus, it can be applied even in pathological cases characterized by discontinuities or lack of derivative information. Using the absolute value instead of the squares in Eq. (9) results in a function, for which other methods (such as the Newton–family methods) fail. The periodic orbits and the computational load reported, are rather indicative, and they are reported to support the claim that the method is efficient. PSO is a stochastic algorithm and this implies that slightly different performance may be achieved, even if the algorithm is initialized with the same initial swarm and velocities. The swarms used in the experiments have been large, but this is inevitable since high accuracy (10^{-10}) is desired.

Further research will consider techniques to improve the convergence properties of the algorithm in high–dimensional cases where high accuracy is desired, as well as hybrid algorithms from combinations of PSO with other powerful methods, such as the generalized Bisection [1], [40], which possess highly desirable theoretical properties.

REFERENCES

- [1] M. Vrahatis, “An efficient method for locating and computing periodic orbits of nonlinear mappings,” *J. Comp. Phys.*, vol. 119, pp. 105–119, 1995.
- [2] G. Birkhoff, “Dynamical systems with two degrees of freedom,” *Trans. Amer. Math. Soc.*, vol. 18, pp. 199–300, 1917.
- [3] T. Bountis and R. Helleman, “On the stability of periodic orbits of two–dimensional mappings,” *J. Math. Physics*, vol. 22, no. 9, p. 1867, 1981.
- [4] J. Greene, “A method for determining a stochastic transition,” *J. Math. Physics*, vol. 20, pp. 1183–1201, 1979.
- [5] R. Helleman, “On the iterative solution of a stochastic mapping,” in *Statistical Mechanics and Statistical Methods in Theory and Applications*, U. Landman, Ed. Plenum, 1977, p. 343.
- [6] M. Hénon, “Numerical study of quadratic area–preserving mappings,” *Quart. Appl. Math.*, vol. 27, pp. 291–311, 1969.
- [7] C. Polymilis, G. Servizi, and C. Skokos, “A quantitative bifurcation analysis of Henon–like 2D maps,” *Cel. Mech. Dyn. Astron.*, vol. 66, pp. 365–385, 1997.
- [8] C. Polymilis, C. Skokos, G. Kollias, G. Servizi, and G. Turchetti, “Bifurcations of beam–beam like maps,” *J. Phys. A*, vol. 33, pp. 1055–1064, 2000.
- [9] C. Skokos, G. Contopoulos, and C. Polymilis, “Structures in the phase space of a four dimensional symplectic map,” *Cel. Mech. Dyn. Astron.*, vol. 65, pp. 223–251, 1997.
- [10] C. Skokos, “Alignment indices: A new, simple method for determining the ordered or chaotic nature of orbits,” *J. Phys. A*, vol. 34, pp. 10029–10043, 2001.

TABLE VI
PERIODIC ORBITS OF THE HÉNON 4D MAP.

Period	Periodic Orbit				Iterations
2	(-1.2773358779,	-0.9999949932,	1.9056707507,	-2.4341853173) [†]	199
3	(-0.2472260058,	-0.1935538651,	1.2285533059,	0.9618081010) [†]	179

TABLE VII
PERIODIC ORBITS OF THE 6D MAP.

Period	Periodic Orbit						Iterations
1	(0.1313051555,	1.0000000000,	0.4999895159	0.9999864919,	0.6313117223,	0.0000000000) [†]	129
1	(0.6341350463,	1.0000000000,	0.4999967282	1.0000000000,	0.1341290822,	0.0000000000) [†]	82
3	(0.2561905777,	0.6666625518,	0.4999941396	1.0000000000,	0.7561962951,	0.6666708609) [†]	132
3	(0.4999920770,	0.3858763098,	0.8858848568	0.3858968564,	0.1141105098,	0.2282217818) [†]	439

- [11] M. Vrahatis and T. Bountis, "An efficient method for computing periodic orbits of conservative dynamical systems," in *Proceedings of the International Conference on Hamiltonian Mechanics, Integrability and Chaotic Behavior*, J. Seimenis, Ed., 1994, pp. 261–274.
- [12] M. Vrahatis, T. Bountis, and M. Kollmann, "Periodic orbits and invariant surfaces of 4-d nonlinear mappings," *Inter. J. Bifurc. Chaos*, vol. 6, pp. 1425–1437, 1996.
- [13] F. Verhulst, *Nonlinear Differential Equations and Dynamical Systems*. Berlin: Springer-Verlag, 1990.
- [14] J. Kennedy and R. Eberhart, *Swarm Intelligence*. Morgan Kaufmann Publishers, 2001.
- [15] —, "Particle swarm optimization," in *Proceedings IEEE International Conference on Neural Networks*, vol. IV. Piscataway, NJ: IEEE Service Center, 1995, pp. 1942–1948.
- [16] K. Parsopoulos and M. Vrahatis, "Recent approaches to global optimization problems through particle swarm optimization," *Natural Computing*, vol. 1, no. 2–3, pp. 235–306, 2002.
- [17] R. Eberhart, P. Simpson, and R. Dobbins, *Computational Intelligence PC Tools*. Academic Press, 1996.
- [18] M. Clerc and J. Kennedy, "The particle swarm—explosion, stability, and convergence in a multidimensional complex space," *IEEE Trans. Evol. Comput.*, vol. 6, no. 1, pp. 58–73, 2001.
- [19] R. Eberhart and Y. Shi, "Comparison between genetic algorithms and particle swarm optimization," in *Evolutionary Programming*, V. Porto, N. Saravanan, D. Waagen, and A. Eiben, Eds. Springer, 1998, vol. VII, pp. 611–616.
- [20] Y. Shi and R. Eberhart, "Parameter selection in particle swarm optimization," in *Evolutionary Programming*, V. Porto, N. Saravanan, D. Waagen, and A. Eiben, Eds. Springer, 1998, vol. VII, pp. 591–600.
- [21] —, "A modified particle swarm optimizer," in *Proceedings IEEE Conference on Evolutionary Computation*. Anchorage, AK: IEEE Service Center, 1998.
- [22] P. Angeline, "Evolutionary optimization versus particle swarm optimization: Philosophy and performance differences," in *Evolutionary Programming*, V. Porto, N. Saravanan, D. Waagen, and A. Eiben, Eds. Springer, 1998, vol. VII, pp. 601–610.
- [23] I. Trelea, "The particle swarm optimization algorithm: Convergence analysis and parameter selection," *Information Processing Letters*, vol. 85, pp. 317–325, 2003.
- [24] J. Kennedy, "The behavior of particles," in *Evolutionary Programming*, V. Porto, N. Saravanan, D. Waagen, and A. Eiben, Eds. Springer, 1998, vol. VII, pp. 581–590.
- [25] K. Parsopoulos, V. Plagianakos, G. Magoulas, and M. Vrahatis, "Stretching technique for obtaining global minimizers through particle swarm optimization," in *Proceedings of the Particle Swarm Optimization Workshop*, Indianapolis (IN), USA, 2001, pp. 22–29.
- [26] K. Parsopoulos and M. Vrahatis, "Initializing the particle swarm optimizer using the nonlinear simplex method," in *Advances in Intelligent Systems, Fuzzy Systems, Evolutionary Computation*, A. Grmela and N. Mastorakis, Eds. WSEAS Press, 2002, pp. 216–221.
- [27] W. Press, S. Teukolsky, W. Vetterling, and B. Flannery, *Numerical Recipes in Fortran 77*. Cambridge University Press, 1992.
- [28] G. Magoulas, M. Vrahatis, and G. Androulakis, "On the alleviation of local minima in backpropagation," *Nonlinear Analysis, Theory, Methods & Applications*, vol. 30, no. 7, pp. 4545–4550, 1997.
- [29] J. Howard and R. Mackay, "Linear stability of symplectic maps," *J. Math. Phys.*, vol. 28, no. 5, pp. 1036–1051, 1987.
- [30] C. Skokos, "On the stability of periodic orbits of high dimensional autonomous hamiltonian systems," *Physica D*, vol. 159, no. 3–4, pp. 155–179, 2001.
- [31] K. Parsopoulos and M. Vrahatis, "Computing periodic orbits of nonlinear mappings through particle swarm optimization," in *Proceedings of the 4th GRACM Congress on Computational Mechanics*, Patras, Greece, 2002.
- [32] S. Rasband, *Chaotic Dynamics of Nonlinear Systems*. New York: Wiley, 1990.
- [33] R. Devaney, "A piecewise linear model for the zones of instability of an area preserving map," *Physica D*, vol. 10, pp. 387–393, 1984.
- [34] J. Maynard Smith, *Mathematical Ideas in Biology*. London: Cambridge University Press, 1968.
- [35] B. Henry, S. Watt, and S. Wearne, "A lattice refinement scheme for finding periodic orbits," *ANZIAM J.*, vol. 42, no. E, pp. C735–C751, 2000.
- [36] E. Lorenz, "Deterministic nonperiodic flow," *J. Atmos. Sci.*, vol. 20, pp. 130–141, 1963.
- [37] O. Rössler, "An equation for continuous chaos," *Phys. Lett. A.*, vol. 57, pp. 397–398, 1976.
- [38] M. Vrahatis, H. Isliker, and T. Bountis, "Structure and breakdown of invariant tori in a 4-d mapping model of accelerator dynamics," *Inter. J. Bifurc. Chaos*, vol. 7, pp. 2707–2722, 1997.
- [39] H. Kantz and P. Grassberger, "Internal Arnold diffusion and chaos thresholds in coupled symplectic maps," *J. Phys. A*, vol. 21, pp. L127–133, 1988.
- [40] M. Vrahatis, "Solving systems of nonlinear equations using the nonzero value of the topological degree," *ACM Trans. Math. Software*, vol. 14, pp. 312–329, 1988.